

# LPS combined with CD47mAb enhances the anti-osteosarcoma ability of macrophages

PENG YUAN<sup>1,2\*</sup>, YUKANG QUE<sup>1\*</sup>, YULEI LIU<sup>1,2</sup>, PENG HE<sup>1</sup>, ZEHAO GUO<sup>1</sup> and YONG HU<sup>1,2</sup>

<sup>1</sup>Department of Orthopedics, Fuyang Hospital of Anhui Medical University, Fuyang, Anhui 236000;

<sup>2</sup>Department of Orthopedics, The First Affiliated Hospital of Anhui Medical University, Hefei, Anhui 230000, P.R. China

Received November 15, 2022; Accepted March 14, 2023

DOI: 10.3892/ol.2023.13777

**Abstract.** Macrophages are abundant in tumor tissues, and they affect the biological properties of tumor cells. The present findings indicated that osteosarcoma (OS) has a high proportion of tumor-promoting M2 macrophages. The CD47 protein can aid tumor cells in their immunological escape. It was identified that CD47 protein is abundant in both clinical OS tissues and OS cell lines. Lipopolysaccharide (LPS) is an activator of Toll-like receptor 4 present on the surface of macrophages, and it induces the polarization towards a pro-inflammatory phenotype; and macrophages of pro-inflammatory phenotype may present antitumor potential. CD47 monoclonal antibody (CD47mAb) can block the CD47-SIRP $\alpha$  signaling pathway, thus enhancing the antitumor ability of macrophages. Immunofluorescence staining confirmed that OS was rich in CD47 protein and M2 macrophages. In the present study, the antitumor potential of macrophages activated using LPS combined with the CD47mAb was assessed. LPS combined with CD47mAb greatly improved macrophages' capacity to phagocytize OS cells, according to the laser confocal experiments and flow cytometry. Furthermore, cell proliferation analysis, cell migration assay and apoptosis determination confirmed LPS-polarized macrophages might efficiently suppress OS cells growth and migration while promoting apoptosis. Taken together, the results of present study demonstrated that LPS combined with CD47mAb enhanced the anti-osteosarcoma ability of macrophages.

## Introduction

Osteosarcoma (OS) is the most common primary bone tumor with an incidence of 0.3 cases/100,000 individuals/year (1,2), with adolescents exhibiting a higher incidence (3). OS is an aggressive cancer characterized by early metastasis, high-grade malignancy, and a poor prognosis (4,5). Treatment strategies for chemotherapy and surgical surgery have enabled the disease-free survival rate to significantly increase to 60% for localized OS (1). However, for patients with axial OS, poor chemosensitivity, or metastatic OS, the prognosis is poor, and the 5-year survival rate is 20-25% (1,6).

Over the past three decades, little progress has been made in the treatment of OS (7). The most recent advances in OS treatment came in the 1980s, when multi-agent chemotherapy was shown to improve overall survival compared with surgery alone (8). Therefore, there is a necessity to investigate OS therapies to offer novel perspectives on therapeutic management. Previous advances in immunotherapy have highlighted new avenues for the treatment of cancer (9). A form of antitumor therapy known as immunotherapy uses the host's own defense mechanisms to combat cancer. Previously, immunotherapy has demonstrated outstanding therapeutic effectiveness against a number of cancers (10). Cancer immunotherapy, which aims to utilize the immune system to combat the tumor, has attracted wide attention (11,12). Immune mechanisms including cytokines, immune checkpoint inhibitors, tumor vaccines and cellular immunotherapy may assist the host's defense against cancer (13,14).

Numerous types of immune cells, including leucocytes of a myeloid lineage, macrophages, helper T cells, cytotoxic T cells, regulatory T cells, B cells, and dendritic cells, reside in the tumor microenvironment (15). *Inter alia*, in the tumor microenvironment, T-lymphocytes and macrophages are the most common immune cells (16,17).

Previously, the research on utilizing macrophages for combating tumors has opened a new window in the field of tumor immunotherapy (18). Macrophages are an important part of the innate immune system and play an essential role in mediating the host's defense against infection and cancer (19). Cancer immunotherapy possesses considerable potential when macrophage-mediated immunity is successfully activated (20). However, by producing a 'do not eat me' signal using CD47 binding to signal regulatory protein  $\alpha$  (SIRP $\alpha$ ) receptors on

---

*Correspondence to:* Dr Yong Hu, Department of Orthopedics, The First Affiliated Hospital of Anhui Medical University, 218 Jixi Road, Shushan, Hefei, Anhui 230000, P.R. China  
E-mail: hy20221017@163.com

\*Contributed equally

**Key words:** osteosarcoma, macrophages, CD47, lipopolysaccharides, immunotherapy

macrophages, tumor cells can prevent against phagocytosis by macrophages (21).

CD47 checkpoint inhibitors have been preliminarily shown to enhance macrophage-mediated phagocytosis of tumor cells, but their effects have been limited (22). Additionally, as with other checkpoint inhibitors, these antagonists need refinements to improve their clinical value rate and objective remission rates (23). Resolving these issues is critical for paving the way for clinical trials on CD47-SIRP $\alpha$  based immunotherapy. Previous tumor immunology research suggested that the reduced effectiveness of CD47-SIRP $\alpha$  blockers may be due to the presence of an immunosuppressive tumor microenvironment (24). Cancer cells in particular release colony-stimulating factors, which polarize tumor-associated macrophages (TAMs) toward the M2 phenotype (25,26). M2 macrophages can recruit regulatory T cells to prevent T cell immunological activation generated by CD47 blockage, as well as enhancing tumor angiogenesis, which can contribute to tumor growth and metastasis. M1 macrophages, conversely, play an important role in innate host defense and tumor cell death by generating reactive oxygen species (ROS), reactive nitrogen, and proinflammatory cytokines (including interleukin-6 and tumor necrosis factor- $\alpha$ ) (27,28). Therefore, stimulating macrophages to polarize towards the M1 phenotype, and increasing the proportion of M1 relative to M2 macrophages in tumor tissues may significantly improve the therapeutic effect of CD47 blockers.

Toll-like receptors (TLRs) are expressed in several tissues and tumors and are important molecules in cancer evasion of immune surveillance (29). Activation of TLRs on macrophages can promote their immune response, including secretion of pro-inflammatory cytokines and enhancement of phagocytosis (30). Therefore, local TLR activation is a popular antitumor immunotherapy (31). Lipopolysaccharides (LPS) are components of the outer wall of the cell wall of Gram-negative bacteria and consist of lipids and polysaccharides (32). LPS is also the main ligand of TLR4, which can effectively activate macrophages to transform towards an M1 phenotype to exert antitumor immune effects (33).

In certain solid tumors, macrophages account for half of the total tumor weight (34). The higher the content of macrophages, the worse the prognosis of tumors, which indicates that macrophages play a very important role in the occurrence and development of tumors (35). Immune targeting of macrophages to tumors has become an encouraging therapeutic strategy. However, there are two major obstacles to effective macrophage activation for antitumor immunotherapy: Promoting M1 transformation of macrophages and anti-SIRP $\alpha$ -CD47 signaling. Therefore, it is hypothesized that simultaneously stimulating macrophages to transform towards an M1 phenotype and blocking the CD47-SIRP  $\alpha$  signaling pathway can significantly improve the antitumor effect of macrophages. In the present study, the combined use of LPS and CD47mAb effectively activated macrophages and significantly improved the anti-OS effect of macrophages, providing novel avenues for tumor immunotherapy.

## Materials and methods

*Human specimens.* In the present study, four OS specimens and one normal bone specimen were obtained from the

Department of Orthopedics, The First Affiliated Hospital of Anhui Medical University, from October 2019 to October 2021. All the OS specimens used were puncture specimens of primary patients (two male and two female; aged between 13 and 55), and the pathological results showed that all of them were common OS. The main feature of common OS is the direct formation of bone-like matrix by tumor cells (36). Regrettably, these OS specimens were not graded, which is a potential limitation to the present study. Specimens were treated in accordance with the guidelines in the Declaration of Helsinki (37). The present study was approved (approval no. PJ2022-10-15) by the Clinical Medical Research Ethics Committee of The First Affiliated Hospital of Anhui Medical University (Fuyang, China).

*Cell culture.* All the cells (RAW264.7, K7M2, U2 OS, MG63) were purchased from Wuhan Procell Life Technology Co., Ltd. Cells were cultured in DMEM (Biological Industries) supplemented with 10% FBS (Wisent Biotechnology), 100 U/ml penicillin (Beyotime Institute of Biotechnology), and 100  $\mu$ g/ml streptomycin (Beyotime Institute of Biotechnology), at 37°C in a humidified incubator supplied with 5% CO<sub>2</sub>. K7M2 OS cells and RAW264.7 macrophages were mainly used for experiments in the present study. K7M2 cells instead of the other OS cell lines were used in combination with RAW264.7 macrophages, because they are both of mouse origin.

*Cell viability.* Cell viability was measured using a Cell Counting Kit-8 (CCK-8) assay. Briefly, K7M2 OS cells were seeded at a density of 1x10<sup>4</sup> cells per well in 96-well plates in quintuplicate and incubated with LPS (0.1  $\mu$ g/ml) (MilliporeSigma), CD47mAb (10  $\mu$ g/ml) (Bio X Cell, clone MIAP301), or a combination of both for 48 h. Subsequently, 10  $\mu$ l of WST-8 reagent (Dalian Meilun Biology Technology Co., Ltd.) was added to each well. After incubation at 37°C for 1 h, the absorbance was measured with an optical density of 450 nm using a Microplate Reader (Tecan Group, Ltd.).

*Cell proliferation analysis.* For cell proliferation analysis, K7M2 cells were pre-stained with 4  $\mu$ M of the cell proliferation dye, CFSE (Invitrogen; Thermo Fisher Scientific, Inc.) according to the manufacturer's instructions. K7M2 cells and RAW264.7 cells were co-cultured in 12-well double-compartment culture plates (LABSELECT). These co-culture systems possess a membrane with a pore diameter of 0.4  $\mu$ m between the upper chamber and the lower chamber of the culture plate, which does not allow cells to pass through, but factors secreted by cells can pass through. A total of 2x10<sup>5</sup> K7M2 cells were added to the lower chamber and 1x10<sup>6</sup> RAW264.7 cells were added to the upper chamber. After incubation with LPS (0.1  $\mu$ g/ml) or CD47mAb (10  $\mu$ g/ml) for 24 h, the K7M2 cells in the lower chamber were collected and washed with PBS. Then the fluorescence intensity was detected by Flow Cytometry (BD Biosciences).

*Phagocytosis assay.* To measure the phagocytic ability of macrophages precisely, K7M2 and RAW264.7 cells were respectively fluorescence-labeled with CFSE (Invitrogen; Thermo Fisher Scientific, Inc.) and the Cell Proliferation Dye eFluor 670 (Invitrogen; Thermo Fisher Scientific, Inc.)

at 37°C for 10 min. After washing with PBS, K7M2 cells were co-cultured with RAW264.7 cells at a ratio of 2:1 and incubated with 0.1 µg/ml LPS, 10 µg/ml CD47mAb, or 0.1 µg/ml LPS + 10 µg/ml CD47mAb for 48 h in a 12-well plate. Subsequently, the cells were collected, washed with PBS twice, and analyzed using a flow cytometer (Beckman Coulter, Inc.). The same method was used to detect the results of the treatment groups with or without 5 µM/1 N-acetyl-cysteine (NAC; Beijing Solarbio Science & Technology Co., Ltd.). The relative phagocytosis index was calculated using FlowJo 10.8.1 (FlowJo LLC) based on the proportion of CFSE and Dye 670 double positive cells.

*Laser confocal microscopy.* To assess phagocytosis visually, K7M2 and RAW264.7 cells were co-cultured as aforementioned. The co-cultured cells were added to a 24-well plate with round coverslips and cultured for 48 h. Cells that had grown on the coverslips were fixed using 4% formaldehyde at room temperature for 30 min, and counterstained using 10 µg/ml DAPI (Beijing Solarbio Science & Technology Co., Ltd.), for 10 min, followed by mounting in anti-fluorescence quencher (Beijing Solarbio Science & Technology Co., Ltd.). Finally, images were obtained by laser confocal microscopy (x63 magnification) (Leica GmbH).

*Histopathological analysis.* A total of four OS specimens and one normal bone tissue specimen were collected and fixed with 4% paraformaldehyde for 24 h. The paraffin-embedded dried tissues were sliced into 4-µm thick slices. For histological analysis, tissue slices were stained with hematoxylin and eosin, and images were captured using a light microscope (x20 magnification).

*Immunofluorescence staining.* The antibodies used for immunofluorescence staining were: CD47 Rabbit pAb (1:100; cat. no. 380870; ZENBIO), CD206 Rabbit mAb (1:100; cat. no. ET1702-04; HUABIO) or CD68 Mouse mAb (1:100; cat. no. 250019; ZENBIO), and Goat Anti-Rabbit Alexa Fluor 488 secondary antibody (1:100; cat. no. M21012M; Abmart Pharmaceutical Technology Co., Ltd.) or Goat Anti-Mouse Alexa Fluor 488 secondary antibody (1:100; cat. no. E-AB-1104; Elabscience Biotechnology, Inc.). For immunohistochemistry, the paraffin-embedded OS tissues and normal bone tissues were dewaxed using dimethyl benzene for 10 min twice and rehydrated in a descending alcohol series. Antigen retrieval was performed by heating at 100°C in citrate buffer for 20 min and blocked using 5% BSA (Bestbio; Nanjing Fengfeng Biomedical Technology Co., Ltd.) for 1 h. Then, the sections were incubated at 4°C overnight with the primary antibody. The following day, the sections were incubated at room temperature for 2 h with the secondary antibody. The nuclei were counterstained with 10 µg/ml DAPI (Beyotime Institute of Biotechnology) at room temperature for 10 min. After each step, the sections were washed with PBS three times. Finally, the sections were mounted in an anti-fluorescence quenching agent, and images were obtained by fluorescence microscopy (x20 magnification). ImageJ 1.53K (National Institutes of Health) was used to analyze the fluorescence area of images. Immunocytochemistry was performed as previously described (38). Briefly, cells were plated in a 24-well plate,

and after adhesion, were fixed with 4% paraformaldehyde at room temperature for 30 min, and immunofluorescence was performed as aforementioned. Images of the cells were captured using a fluorescence microscope (x20 magnification).

*Western blotting.* Western blot analysis was performed as previously described (39). Briefly, RIPA lysis Buffer (Beyotime Institute of Biotechnology) was used to lyse tumor cells and extract proteins. Lysates from each sample were denatured and then loaded (30 µg/lane; protein concentration determined by a DeNovix DS-11 spectrophotometer) onto 4-20% SDS-gels, resolved using SDS-PAGE, transferred to PVDF membranes, and blocked in non-fat milk at room temperature for 1.5 h, then incubated with either NOS2 Rabbit pAb (1:200; cat. no. WL0992a; Wanleibio Co., Ltd.) or rabbit anti-β-actin (1:1,000; cat. no. AF7018; Affinity Biosciences) at 4°C overnight. The following day, the membrane was incubated with horseradish peroxidase-conjugated secondary antibody (1:10,000; cat. no. S0001; Affinity Biosciences) at room temperature for 2 h. Finally, signals were visualized using ECL super western blot detection reagent (Abmart Pharmaceutical Technology Co., Ltd.). The relative expression of each protein was calculated using ImageJ (version 1.53k; National Institutes of Health) with β-actin as an internal reference.

*Cell migration assay.* Cell migration assays were performed using 24-well Transwell plates with 8-µm pores (Corning, Inc.). A total of 2x10<sup>5</sup> K7M2 cells in 200 µl serum-free DMEM was added to the upper chamber, and 600 µl supplemented media containing 1x10<sup>5</sup> RAW264.7 cells, or no cells as a control, was added to the lower chamber. After 24 h of incubation with LPS (0.1 µg/ml) or CD47mAb (10 µg/ml), K7M2 cells were fixed using 4% paraformaldehyde at room temperature for 30 min and stained using 0.1% crystal violet for 30 min at room temperature. Three visual fields were randomly selected to count migratory cells under a fluorescence microscope (x40 magnification).

*ELISA.* RAW264.7 cells were incubated with or without LPS (0.1 µg/ml) or CD47mAb (10 µg/ml) for 24 h. The levels of TNF-α in the cell culture supernatant of cells subjected to different treatments were measured using a specific ELISA kit (cat. no. m1002095-2; Shanghai Enzyme-linked Biotechnology Co., Ltd.) according to the manufacturer's instructions.

*Detection of NO.* RAW264.7 cells were incubated with or without LPS (0.1 µg/ml) or CD47mAb (10 µg/ml) for 24 h. NO was measured using a commercial kit (cat. no. BC1470; Beijing Solarbio Science & Technology Co., Ltd.) according to the manufacturer's protocol. Absorbance was measured at an optical density of 550 nm using a microplate reader.

*Detection of CD86 and ROS levels.* K7M2 cells and RAW264.7 cells were co-cultured as aforementioned for the cell proliferation analysis, except with 2x10<sup>6</sup> RAW264.7 cells. After incubation with LPS (0.1 µg/ml) or CD47mAb (10 µg/ml) for 24 h, the macrophages in the lower chamber were collected and washed with PBS (500 x g, 4°C, 5 min). The washed cells were resuspended in 50 µl PBS and incubated with 1 µl CD86 flow antibody (cat. no. 564198; BD Biosciences) for 30 min at

4°C, and subsequently washed with PBS. CD86 expression was determined using flow cytometry. Cells were collected and ROS levels were measured using an ROS detection kit (cat. no. S0033S; Beyotime Institute of Biotechnology) according to the manufacturer's protocol.

**Apoptosis determination.** In order to verify the apoptotic effect of LPS and CD47mAb on OS cells, K7M2 OS cells were cultured with LPS or CD47mAb in 12-well plates for 48 h. Then, K7M2 cells were collected and washed with PBS (500 × g, 4°C, 5 min), and the proportion of apoptosis was detected by Flow Cytometry (BD Biosciences). Next, to verify the effect of polarized macrophages on the apoptosis of OS cells, K7M2 cells and RAW264.7 cells were co-cultured in 12-well double-compartment culture plates (LABSELECT). A total of 2 × 10<sup>5</sup> K7M2 cells were added to the lower chamber and 1 × 10<sup>6</sup> RAW264.7 cells were added to the upper chamber. After incubation with LPS (0.1 μg/ml) or CD47mAb (10 μg/ml) for 24 h, the K7M2 cells in the lower chamber were collected and washed with PBS. Apoptosis was measured using Annexin V-FITC (cat. no. BB-4101-100T; BestBio; Nanjing Fengfeng Biomedical Technology Co., Ltd.) according to the manufacturer's protocol. The apoptosis data was calculated using FlowJo 10.8.1 (FlowJo LLC).

**Statistical analysis.** All experiments were repeated at least three times, and data are presented as the mean ± SD. The data in Fig. 1 were analyzed using one-way ANOVA, followed by Dunnett's test. The data in Fig. 3E were analyzed using unpaired Student's t-test. The data in Figs. 4H and S2D were analyzed using one-way ANOVA, followed by LSD test. Other data were analyzed using one-way ANOVA, followed by Tukey's post hoc test. All statistical analysis was performed using GraphPad Prism 9.0.2 (Dotmatics). P < 0.05 was considered to indicate a statistically significant difference.

## Results

**CD47 and TAMs are found in human OS.** The expression of CD47 in OS is a prerequisite for the use of CD47mAb as an immunotherapy in the treatment of OS. Using immunofluorescence labeling, it was demonstrated that the expression levels of CD47 in OS patient specimens were significantly greater than that in normal bone tissues (Fig. 1A and B). At the same time, immunofluorescence staining showed that the expression of the M2 TAMs markers, CD68 and CD206, in OS specimens were significantly higher than those in normal bone tissues (Fig. 1A, C and D). This demonstrated that M2 TAMs are abundantly present in OS. Taken with previous studies, M2 TAMs will promote tumor development (28). However, due to the low incidence of OS, specimen collection is difficult, thus only four OS samples were studied. This may bring more errors to the experimental results. More samples will be collected in the authors' future research work. In OS tissues, tumor cells and various immune cells are intertwined, and the components are unevenly distributed, thus the immunofluorescence staining results of different samples are quite different. Cell immunofluorescence labeling was also used to validate the expression of CD47 in U-2 OS, MG63 and K7M2 OS cell lines. The results revealed that the expression of CD47

is abundant in U-2 OS, MG63, and K7M2 cell lines, using cell immunofluorescence staining (Fig. 1E). The pathological analysis of normal bone and OS tissues using H&E staining is shown in Fig. S1.

**Effect of LPS and CD47mAb on macrophage activation.** Different subtypes of macrophages express different proteins and cytokines (40). To verify the activation effect of LPS (0.1 μg/ml) and CD47mAb (10 μg/ml) on macrophages, the expression of M1 macrophage-related proteins was analyzed in RAW264.7 cells that were co-cultured with LPS, CD47mAb or both. The results of western blot analysis demonstrated that LPS could increase the expression of NOS2 in macrophages, but CD47mAb had no such effect (Fig. 2A and B). The supernatant from the macrophage cultures was collected from the different treatment groups, and the content of NO and TNF-α was measured; the results (Fig. 2C and D) agreed with the results of the western blot analysis. To further verify the effect of LPS (0.1 μg/ml) on polarization and CD47mAb (10 μg/ml) on the proportion of each macrophage phenotype in the macrophage-tumor co-culture system, a co-culture chamber was used as shown in Fig. 2E to separate tumor cells from macrophages. After 24 h of culturing, RAW264.7 cells were collected, and the expression of CD86, a surface marker of M1 macrophages, and ROS, an important product of macrophage activation, was detected by flow cytometry. The results (Fig. 2F-I) also revealed that LPS could effectively activate macrophages and transform them into the antitumor M1 phenotype. These results suggested that LPS can successfully polarize macrophages, but compared with LPS alone, the combination of LPS and CD47mAb has no advantage in stimulating macrophage polarization. Further experiments showed that CD47mAb combined with LPS has a significant advantage in promoting the phagocytosis of macrophages (Fig. 3). In the present study, the drug concentration of CD47mAb used in this experiment refers to other relevant studies (41). The concentration of LPS was determined by simple pre-experiment. The pre-experiment, including Elisa and CCK-8 assays, showed that LPS (0.1 μg/ml) could effectively stimulate macrophage polarization and without obvious cytotoxicity (data not shown).

**Impact of LPS and CD47mAb on phagocytosis.** As a part of the immune system, the powerful phagocytosis executed by macrophages plays an important role in clearing tumorigenic cells (42). In view of the polarization of macrophages induced by LPS and the blocking effect of CD47mAb on the CD47-SIRPα signaling pathway, the combined effect of both on tumor phagocytosis of macrophages was investigated next. CFSE pre-stained K7M2 and Dye 670 pre-stained RAW264.7 cells were co-cultured in a 2:1 ratio and incubated with LPS, CD47mAb, or LPS and CD47mAb for 48 h. Then the phagocytic function of macrophages was observed using laser confocal microscopy. The results showed that the proportion of phagocytic macrophages, when treated with the combination of LPS and CD47mAb, was significantly higher than that in the control group and in the group treated with LPS or CD47mAb alone (Fig. 3A and B). To obtain more accurate data, the experiments were repeated and assessed using flow cytometry. As demonstrated in Fig. 3C, the results of the flow

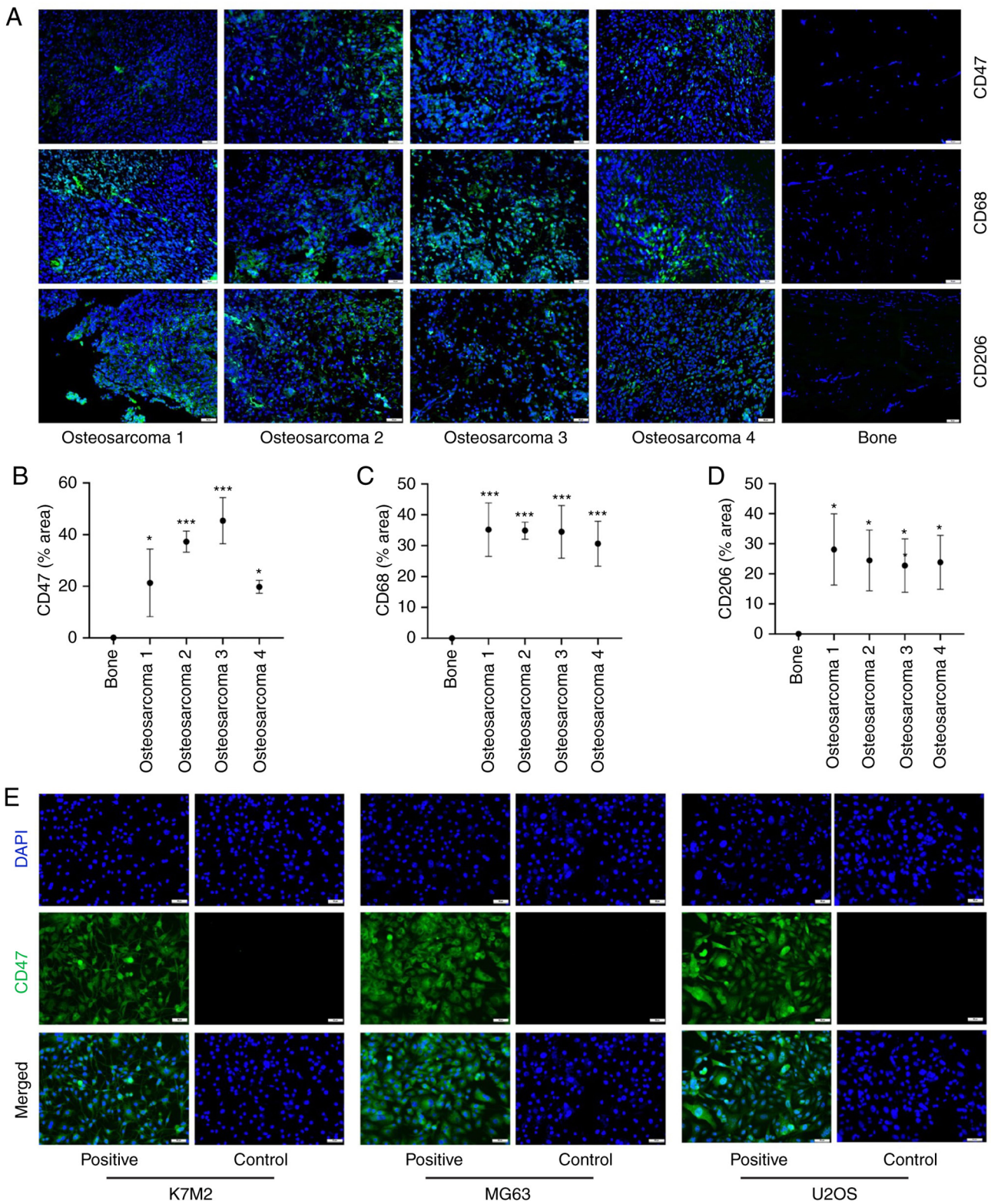


Figure 1. CD47 expression and tumor-associated macrophage presence is abundant OS tissues. (A) CD47, CD68 and CD206 immunofluorescence staining of four human OS samples, and a normal bone sample. Scale bar, 50  $\mu$ m. (B-D) Corresponding quantitative area of CD47, CD68 and CD206 staining in one bone tissue, and three OS samples were measured over three high-power fields of view using ImageJ (magnification, x20). (E) CD47 immunofluorescence staining of three different OS cell lines, and a control sample without the fluorescent secondary antibody. Magnification, x20. Data are presented as the mean  $\pm$  SD of three independent experiments. \* $P$ <0.05 and \*\*\* $P$ <0.001 vs. Bone. OS, osteosarcoma.

cytometric analysis were consistent with those of the confocal microscopy results. This suggested that stimulating macrophage polarization and blocking the CD47-SIRP $\alpha$  signaling pathway at the same time can more effectively overcome

tumor immune escape. ROS play a crucial function in controlling macrophage phagocytosis (43). Thus, a ROS scavenger, N-acetyl-cysteine, was used to scavenge the ROS produced by the LPS-stimulated macrophages, and this resulted in a

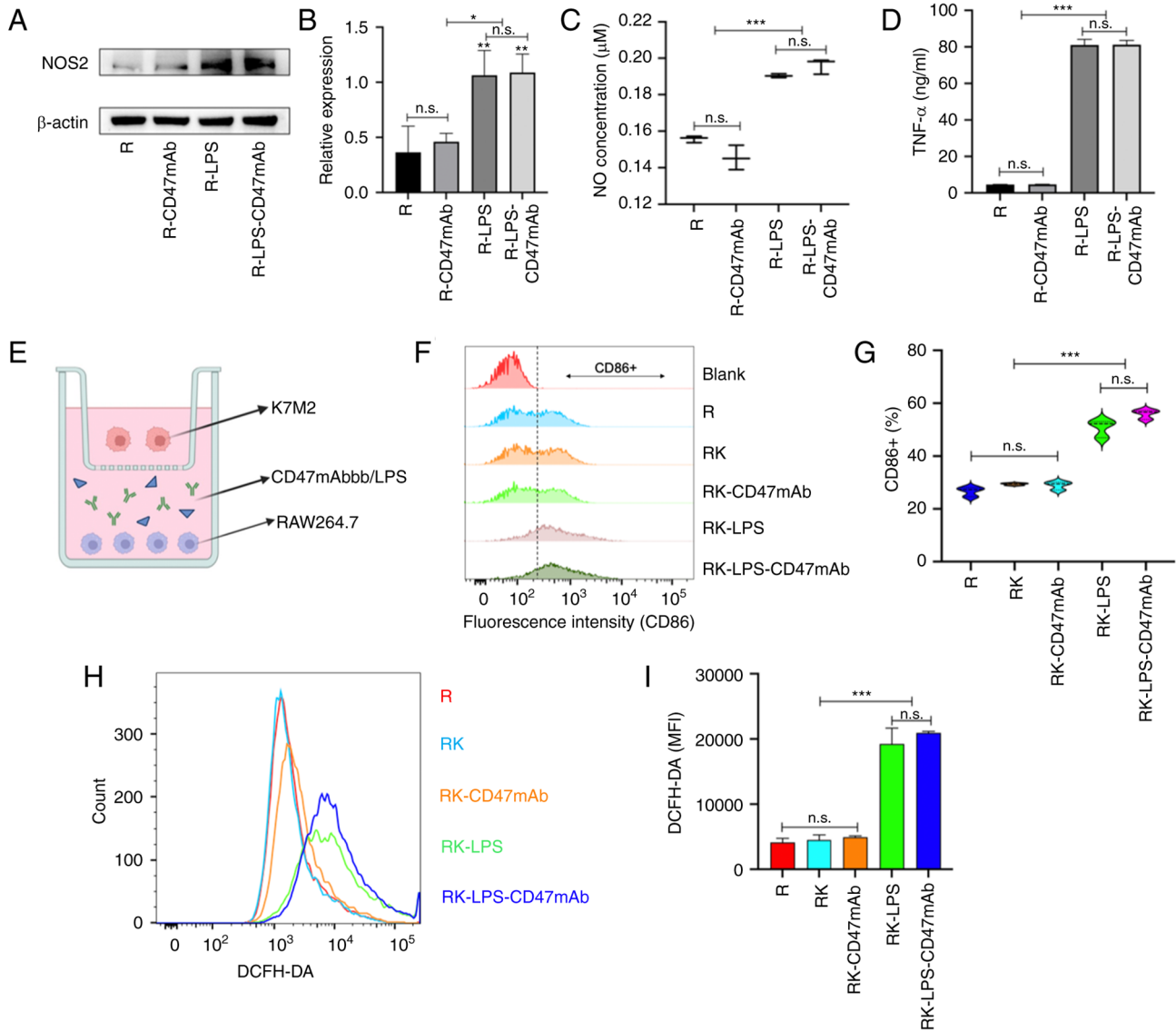


Figure 2. Effect of LPS and CD47mAb on macrophage activation. (A) Western blot analysis and (B) densitometric analysis was used to confirm the expression of NOS2 in RAW264.7 cells treated as indicated. (C and D) NO and TNF- $\alpha$  content in the supernatant of RAW264.7 treated as indicated. (E) Co-culture model of the K7M2 and RAW264.7 cells. (F and G) Flow cytometry was used to measure CD86 expression in the RAW264.7 cells. (H and I) The ROS content in RAW264.7 cells in the different treatment groups was detected using flow cytometry. Data are presented as the mean  $\pm$  SD of three repeats. \* $P$ <0.05, \*\* $P$ <0.01 and \*\*\* $P$ <0.001. n.s., not significant; NO, nitric oxide; TNF- $\alpha$ , tumor necrosis factor  $\alpha$ ; LPS, lipopolysaccharide; CD47mAb, CD47 monoclonal antibody; ROS, reactive oxygen species; MFI, mean fluorescence intensity; R, RAW264.7; K, K7M2; RK, RAW264.7 + K7M2.

significant decrease in the phagocytic ability of macrophages (Fig. 3D). Thus, ROS plays a crucial role in macrophage phagocytosis.

**Combined effect of LPS and CD47mAb on inhibition of OS growth.** The anti-OS regimen of LPS combined with CD47mAb effectively activated macrophages, and induced the release a large number of cytotoxic factors including ROS, NO and TNF- $\alpha$  from macrophages (Fig. 2). Therefore, it was hypothesized that LPS combined with CD47mAb would both promote the phagocytosis of OS cells by macrophages, and also inhibit the proliferation of tumor cells by macrophages. First, CCK-8 assays were used to detect the toxicity of LPS and CD47mAb on K7M2 cells in the absence of macrophages. The results revealed that low concentrations of LPS and CD47mAb had no significant effect on the viability of K7M2

cells (Fig. 4A-C). Next, CFSE pre-stained K7M2 cells were co-cultured with RAW264.7 cells in the co-culture chamber (Fig. 4D), and the co-cultured cells were treated with LPS or CD47mAb for 24 h. Then, the fluorescence intensity of CFSE-K7M2 was detected by flow cytometry. CFSE dye is used to detect proliferation, and the fluorescence intensity of CFSE-labeled cells is halved every time a stained cell is divided. The fluorescence of K7M2 cells cultured alone was the weakest compared with that of K7M2 cells co-cultured with macrophages (Fig. 4E and F), indicating that the number of divisions of K7M2 cells was higher in this group. In the co-culture system, the fluorescence intensity of the groups treated with LPS or LPS-CD47mAb was the highest (Fig. 4E and F), indicating that the corresponding groups had the lowest number of divisions, whereas CD47mAb did not have a notable effect on tumor cell division. This result is

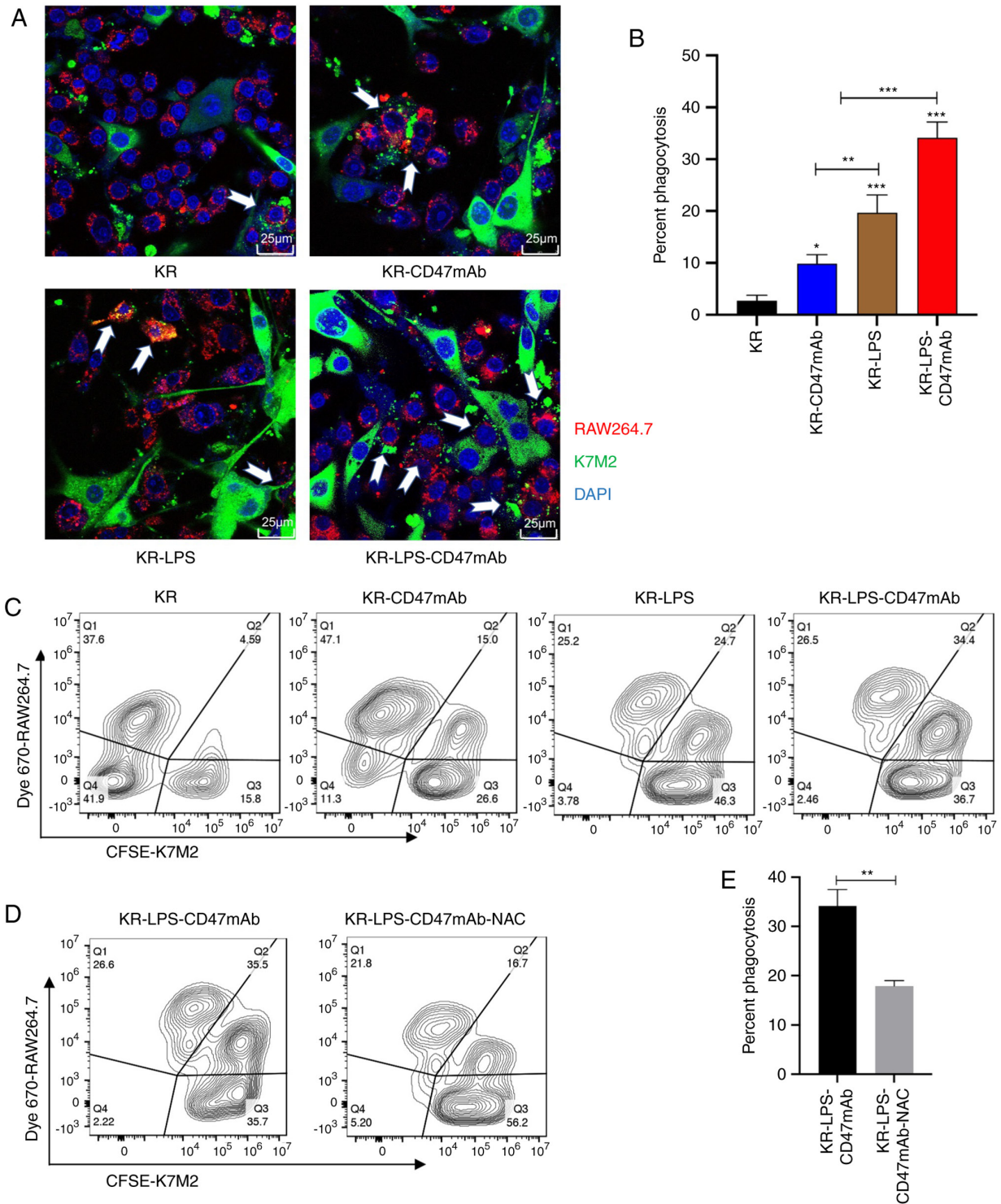


Figure 3. Impact of LPS and CD47mAb on phagocytosis. (A) CFSE-labeled K7M2 cells were co-cultured with Dye 670-labeled RAW264.7 cells and treated with LPS (0.1  $\mu\text{g/ml}$ ), CD47mAb (10  $\mu\text{g/ml}$ ), or both. Phagocytosis was analyzed using a laser confocal microscopy. White arrows indicate K7M2 cells phagocytized and digested by macrophages (magnification, x63) and (B) corresponding quantitative phagocytosis. Phagocytosis was calculated as follows: (number of macrophages with phagocytized cancer cells/total number of macrophages)  $\times 100\%$ . (C) CFSE pre-labeled K7M2 cells were co-cultured with Dye 670 pre-stained RAW264.7 cells and incubated with LPS (0.1  $\mu\text{g/ml}$ ), CD47mAb (10  $\mu\text{g/ml}$ ), or both; phagocytosis (CFSE and Dye 670 positive cells) was analyzed by flow cytometry. (D) The rate of phagocytosis following treatment with the ROS scavenger NAC in the co-culture system was detected using flow cytometry. (E) Quantification of phagocytosis (CFSE and Dye 670 positive cells). Data are presented as the mean  $\pm$  SD of three independent repeats. \* $P < 0.05$ , \*\* $P < 0.01$  and \*\*\* $P < 0.001$  vs. KR or as otherwise indicated. K, K742; R, RAW264.7; KR, K7M2 + RAW264.7; NAC, n-acetyl-cysteine; ROS, reactive oxygen species; LPS, Lipopolysaccharide; CD47mAb, CD47 monoclonal antibody.

consistent with the fact that LPS promotes the M1 polarization of macrophages. The results showed that macrophages could inhibit the proliferation of tumor cells, and the inhibitory

effect of polarized macrophages on tumor proliferation was significantly enhanced. To more intuitively observe the inhibition of tumor proliferation by macrophages, K7M2 cells were

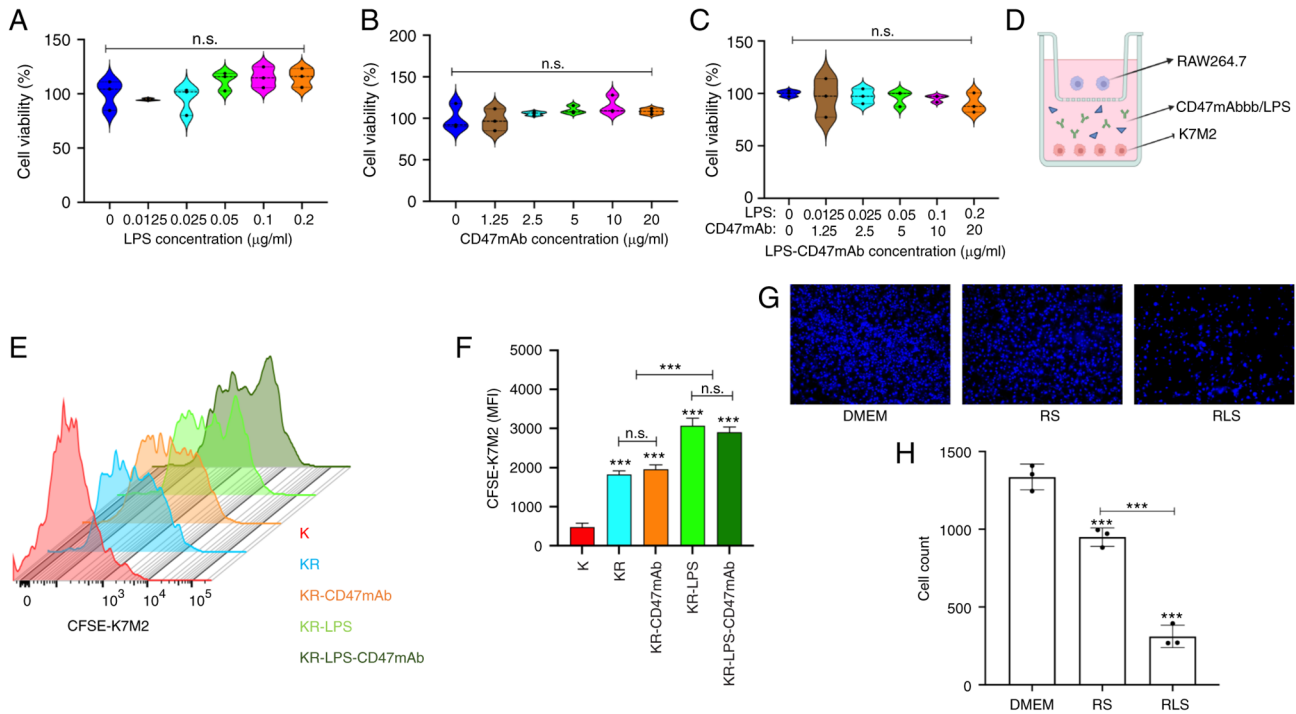


Figure 4. LPS combined with CD47mAb inhibits the proliferation of OS cells. (A-C) K7M2 cells were incubated with LPS, CD47mAb, or both combined for 48 h and the cell viability was analyzed using a Cell Counting Kit-8 assay. (D) Schematic diagram of the K7M2 and RAW264.7 co-culture system. (E and F) CFSE pre-stained K7M2 and RAW264.7 cells were co-cultured and co-incubated with LPS, CD47mAb, or both for 24 h. The fluorescence intensity of CFSE-K7M2 cells was detected by flow cytometry. The greater the degree of proliferation, the weaker the fluorescence intensity was. (G and H) RAW264.7 cells were incubated with or without LPS for 24 h, after which cells were cultured in serum-free DMEM for 24 h. The supernatant was collected and used to culture K7M2 cells for 24 h. Subsequently, K7M2 cells were stained with DAPI and images were captured. Magnification, x10. DMEM group, K7M2 cells cultured with DMEM; RS, K7M2 cells cultured in RAW264.7 cell culture supernatant; RLS, K7M2 cells cultured in RAW264.7 cell culture supernatant treated with 0.1 μg/ml LPS. Data are presented as the mean ± SD of three independent experiments. \*\*\* $P < 0.001$  vs. K or as otherwise indicated. n.s., not significant; K, K7M2; R, RAW264.7; KR, K7M2 + RAW264.7; LPS, lipopolysaccharide; OS, osteosarcoma; CD47mAb, CD47 monoclonal antibody; MFI, Mean Fluorescence Intensity.

cultured in serum-free DMEM and RAW264.7 cell culture supernatant under different treatment conditions. After 24 h, K7M2 cells were stained with DAPI, and the results were observed using a fluorescence microscope (Fig. 4G and H). In addition, the results of apoptosis experiments demonstrated that LPS could significantly promote the apoptosis of osteosarcoma cells induced by macrophages (Fig. S2).

**Activated macrophages inhibit migration of OS cells.** OS is highly malignant and metastasizes early (44). Macrophages are an important part of the immune system, and it is of great significance to study their role in tumor metastasis. The effects of LPS and CD47mAb on the migratory ability of K7M2 cells were evaluated by Transwell assay. The results showed that compared with the control group, LPS and CD47mAb alone or combined did not significantly alter the migratory ability of K7M2 cells (Fig. 5A and B). Next, macrophages were added to the lower chamber of the Transwell insert to observe their ability to alter the migration of K7M2 cells in the different treatment groups. As demonstrated in Fig. 5C and D, macrophages effectively inhibited the migratory ability of OS cells. When LPS was added to the co-culture system, the migratory ability of K7M2 cells decreased significantly, which indicated that LPS could enhance the inhibition of tumor migration by macrophages, but CD47mAb did not have this effect. This

result is consistent with the fact that LPS can promote the polarization of macrophages. Therefore, the significant inhibitory effect of macrophages on tumor migration when treated with a combination of LPS and CD47mAb was primarily due to the effect of LPS on the polarization of macrophages (Fig. 5C and D).

## Discussion

There is mounting evidence that the immune system may be commandeered to prevent carcinogenesis and eliminate tumor cells (45,46). In cancer treatment, immunotherapy using targeted checkpoint preparations has made notable progress (47). CTLA4 antibodies, PD-1/PD-L1 antibodies, as well as CAR-T and TCR-T, have proven instrumental in improving the management of cancer, and all of these utilize T cells (48,49). Although immunotherapy based on T cells has proven valuable, it has limitations, such as its muted effect in solid tumors; most patients with PD-1/PDL-1 antibodies used to treat solid tumors do not respond (50-53). The poor effect of PD-1/PDL-1 antibody in solid tumors may be related to the low expression of PDL-1 in solid tumors (54). In addition, the dense tumor microenvironment of solid tumors limits the penetration of PDL-1 antibodies with high molecular weight into the tumor stroma (55). Certain experiments have shown that the drug conjugate of PDL-1 antibody can achieve the

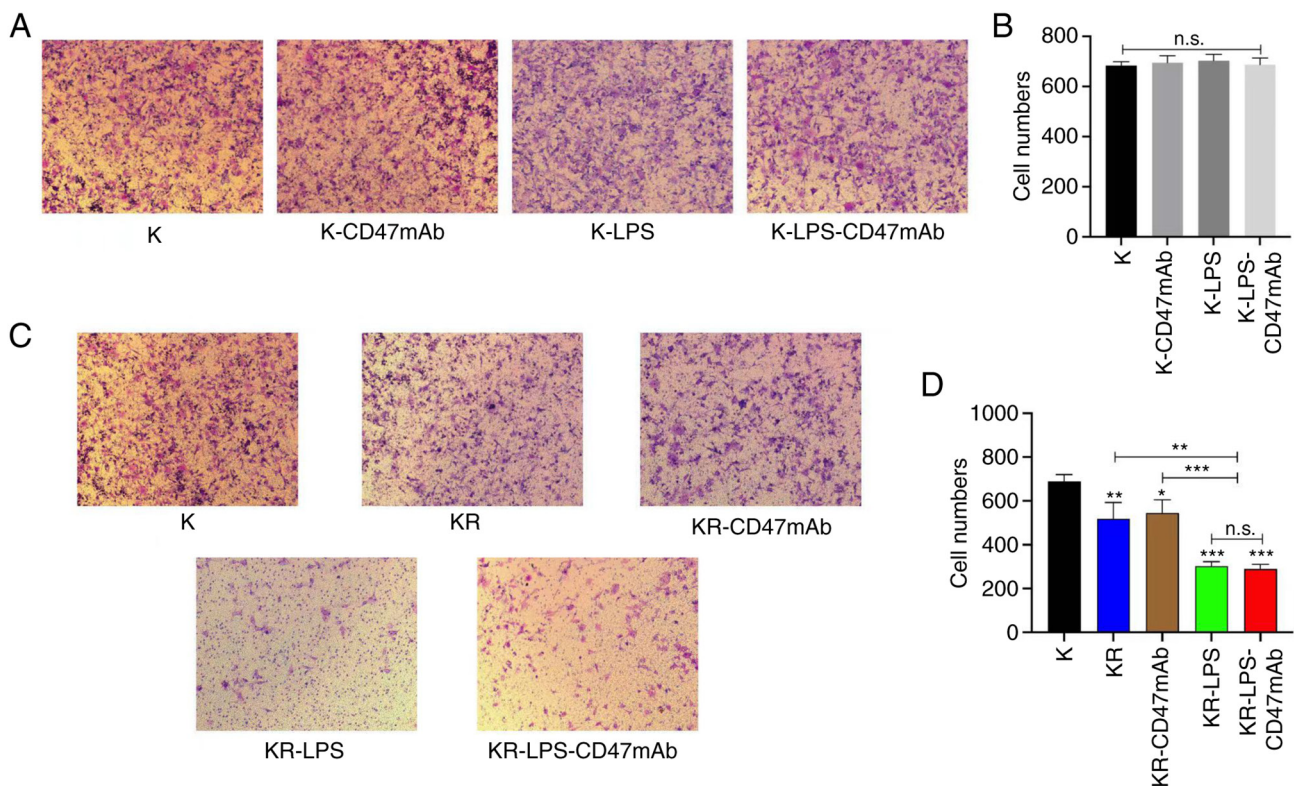


Figure 5. Activated macrophages inhibit the migration of OS. (A) The serum-free medium containing K7M2 was added to the upper chamber of the Transwell inserts, and the lower chamber was filled with supplemented media. After 24 h of incubation with LPS or CD47mAb, migratory cells were stained and observed. (B) Quantitative analysis of the Transwell migration assays shown in panel A. (C) The serum-free media containing K7M2 was added to the upper chamber of the Transwell inserts, and the lower chamber was filled with supplemented media, with or without RAW264.7 cells; migratory cells were stained and observed. Magnification,  $\times 40$ . (D) Quantitative analysis of the Transwell migration assay shown in panel C. Data are presented as the mean  $\pm$  SD of three independent experiments. \* $P < 0.05$ , \*\* $P < 0.01$  and \*\*\* $P < 0.001$  vs. K or as otherwise indicated. n.s., not significant; K, K7M2; R, RAW264.7; KR, K7M2 + RAW264.7; LPS, lipopolysaccharide; OS, osteosarcoma; CD47mAb, CD47 monoclonal antibody.

purpose of chemically guided immunotherapy by destroying the tumor matrix (56).

Thus, a novel avenue in the field of immunotherapy is required to address this. Although the non-specific immune response, represented by macrophages, has poor specificity, it has a significantly wider coverage. CD47 is expressed on the surface of tumor cells and its activation promotes tumor progression and tumor immune escape. Blocking CD47 is considered to be another method of immune checkpoint therapy (57). CD47mAb combined with anti-GD2 has made notable progress in the treatment of tumors (58). However, the antitumor effect of CD47mAb alone is not significant (22,59). In recent years, combinatorial immunotherapy has attracted significant attention due to its additive or synergistic effects in tumor therapy (60,61). The present study suggested that the combination of macrophage activator LPS and CD47mAb can enhance the activation of macrophages and exerts a stronger antitumor effect than either used alone. A schematic illustration of LPS combined with CD47mAb as a hypothetical method of immunotherapy in OS is presented in Fig. 6.

OS is a highly malignant tumor with a very low cure rate and it poses a significant burden on patients and society (4). Thus, there is an urgent need of a more effective and economical treatment. The present results demonstrated the efficacy of a novel combinatorial antitumor immunotherapeutic approach using LPS and CD47mAb for the treatment of OS. This research provides an effective and feasible innovative idea for

the treatment of OS. The results showed that low doses of LPS and CD47mAb had almost no effect on the viability of OS. In a co-culture system, LPS combined with CD47mAb significantly enhanced the phagocytosis of macrophages on OS cells and reduced the proliferation of OS cells. There are two primary causes underlying this: First, LPS polarizes macrophages to an antitumor phenotype, which exhibit increased tumor cytotoxicity and phagocytosis; second, CD47mAb blocks the CD47-SIRP $\alpha$  signaling pathway by blocking CD47 signal proteins on the surface of OS cells, thus further enhancing the recognition and phagocytosis by macrophages to OS cells. In the present study, it was identified that macrophages and tumor cells come into contact with each other, and CD47mAb and LPS play a joint role in promoting the phagocytosis of OS cells by macrophages. Furthermore, it was revealed that macrophages inhibit OS cells mainly through indirect actions, such as the release of TNF- $\alpha$ , ROS and NO. Therefore, the combined use of LPS and CD47mAb fully activated the antitumor effect of macrophages.

The combined effect of CD47mAb and LPS is mainly shown in promoting the phagocytosis of macrophages. When CD47mAb is used in combination with LPS, LPS is responsible for polarizing macrophages and CD47mAb is responsible for blocking CD47-SIRP $\alpha$  signaling pathway. It was also shown that whether LPS was combined with CD47mAb or used alone, the anti-OS effect of macrophages was higher than that of CD47mAb alone. This is because LPS can polarize

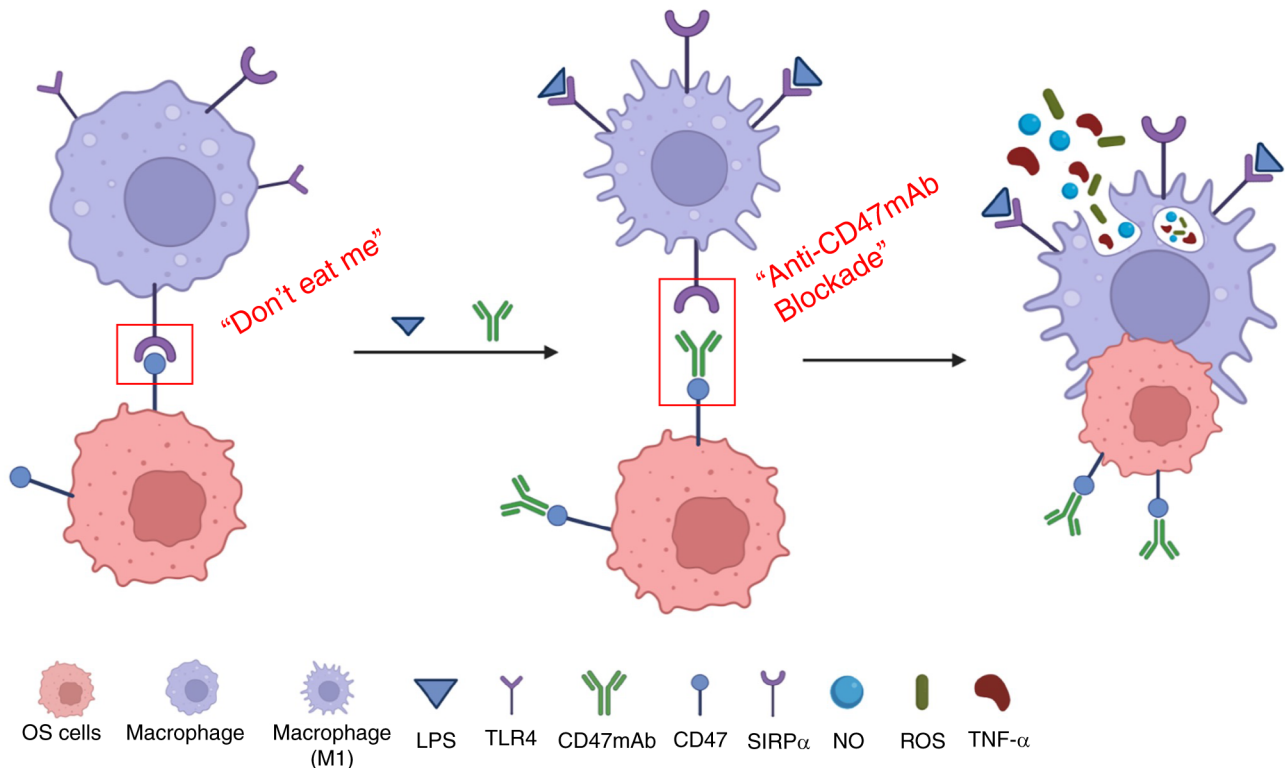


Figure 6. Schematic illustration of LPS combined with CD47mAb as a hypothetical method of immunotherapy in OS. CD47 is present on the surface of OS cells and its binding to SIRP $\alpha$  on macrophages inhibits phagocytosis by macrophages. Blocking the interaction between CD47 and SIRP $\alpha$  with CD47mAb prevents the inhibition of phagocytosis by macrophages, increasing phagocytosis of the OS cells. LPS can bind to TLR4 receptors on macrophages and promote macrophages to polarize towards an M1 phenotype. M1 macrophages exhibit a more potent phagocytotic ability and secrete an increased quantity of antitumor factors, including TNF- $\alpha$ , NO and ROS. LPS and CD47mAb may thus have a significant synergistic effect in tumor immunotherapy. OS, osteosarcoma; NO, nitric oxide; TNF- $\alpha$ , tumor necrosis factor  $\alpha$ ; LPS, lipopolysaccharide; CD47mAb, CD47 monoclonal antibody; ROS, reactive oxygen species; TLR4, toll-like receptors 4; SIRP $\alpha$ , signal regulatory protein  $\alpha$ .

macrophages, promote macrophages to release various cytokines, and then indirectly inhibit the activity of OS cells. However, CD47mAb does not have this effect. This showed that the antitumor effect of macrophages depends, to a large extent, on phenotypic transformation; that is, M1 macrophages are the primary mediators of tumor immunity. These results provide a favorable direction for future research on tumor immunity.

In the present study, there were a large number of M2 TAMs in the tumor tissues of patients with OS, consistent with a previous study (62). As M2 macrophages promote tumor development, they cannot engulf tumor cells, thus only M1 macrophages exhibit an antitumor effect (27,40), and thus it is hypothesized that this may be an important reason underlying the poor effect of CD47mAb alone. Increasing the proportion of M1 macrophages in the tumor tissues and reducing the proportion of M2 macrophages is an effective method to increase the antitumor effects of macrophages. To the best of our knowledge, although LPS has been used to stimulate macrophage polarization in several studies, the present study is the first to use LPS and CD47mAb together to treat OS.

Several studies have confirmed that stimulating macrophages to polarize towards an M1 phenotype can inhibit tumor growth (63,64). However, the immune escape exhibited by tumors significantly limits the effects of M1 macrophages. In the current study, LPS with CD47mab

were used together to inhibit tumor growth and effectively prevent the immune escape of tumor cells. The actions of these two treatments complement each other and promote the antitumor effects of M1 macrophages. In addition, the present study did show that macrophages activated by LPS can inhibit the migration of OS cells and promote their apoptosis. Of course, in the cell migration assays, the apoptosis of OS cells induced by macrophages will reduce the number of OS cells, which has a potential impact on the results of the migration assays.

CD47mAb promotes the phagocytosis of tumor cells by macrophages, and inhibition of CD47 can effectively enhance the antitumor effects of macrophages by directly activating cytotoxic T cells in immune-active mice (22,65). Animal experiments were not performed in the present study, which may be considered a limitation. In future studies, the efficacy of LPS combined with CD47mAb in animal models will be determined as well as its other roles in the tumor microenvironment.

In conclusion, the results of the present study highlight the combined effect of simultaneously stimulating macrophage polarization and blocking tumor immune escape pathways in tumor immunotherapy. This new strategy of tumor immunotherapy may serve as a reference for the development of clinical treatments against OS, and may also provide novel immunotherapeutic approaches for the management of several types of cancer.

## Acknowledgements

Not applicable.

## Funding

The present study was supported by the Major Project of Natural Science Foundation of Anhui Province Colleges and Universities (grant no. KJ2020ZD17).

## Availability of data and materials

The datasets used and/or analyzed during the current study are available from the corresponding author on reasonable request.

## Authors' contributions

YH, PY and YQ conceived the study. PY, YQ and YL performed the experiments and data analyses. PH and ZG contributed to performing the experiments, data acquisition and data analysis. YH, PY and YQ wrote the manuscript. YH, PY and YQ confirm the authenticity of all the raw data. All authors revised the manuscript. All authors have read and approved the final manuscript.

## Ethics approval and consent to participate

The present study was reviewed and approved (approval no. PJ2022-10-15) by the Clinical Medical Research Ethics Committee of The First Affiliated Hospital of Anhui Medical University (Hefei, China). Written informed consent for participation was not required for the present study in accordance with the national legislation and the institutional requirements.

## Patient consent for publication

Not applicable.

## Competing interests

The authors declare that they have no competing interests.

## References

- Casali PG, Bielack S, Abecassis N, Aro HT, Bauer S, Biagini R, Bonvalot S, Boukovinas I, Bovee JVMG, Brennan B, *et al*: Bone sarcomas: ESMO-PaedCan-EURACAN clinical practice guidelines for diagnosis, treatment and follow-up. *Ann Oncol* 29 (Suppl 4): iv79-iv95, 2018.
- Zoumpoulidou G, Alvarez-Mendoza C, Mancusi C, Ahmed RM, Denman M, Steele CD, Tarabichi M, Roy E, Davies LR, Manji J, *et al*: Therapeutic vulnerability to PARP1,2 inhibition in RB1-mutant osteosarcoma. *Nat Commun* 12: 7064, 2021.
- Whelan J, McTiernan A, Cooper N, Wong YK, Francis M, Vernon S and Strauss SJ: Incidence and survival of malignant bone sarcomas in England 1979-2007. *Int J Cancer* 131: E508-E517, 2012.
- Ta HT, Dass CR, Choong PFM and Dunstan DE: Osteosarcoma treatment: State of the art. *Cancer Metastasis Rev* 28: 247-263, 2009.
- He P, Xu S, Guo Z, Yuan P, Liu Y, Chen Y, Zhang T, Que Y and Hu Y: Pharmacodynamics and pharmacokinetics of PLGA-based doxorubicin-loaded implants for tumor therapy. *Drug Deliv* 29: 478-488, 2022.
- Whelan JS and Davis LE: Osteosarcoma, chondrosarcoma, and chordoma. *J Clin Oncol* 36: 188-193, 2018.
- Lagmay JP, Krailo MD, Dang H, Kim A, Hawkins DS, Beaty O III, Widemann BC, Zwerdling T, Bomgaars L, Langevin AM, *et al*: Outcome of patients with recurrent osteosarcoma enrolled in seven phase II trials through children's cancer group, pediatric oncology group, and children's oncology group: learning from the past to move forward. *J Clin Oncol* 34: 3031-3038, 2016.
- Link MP, Goorin AM, Miser AW, Green AA, Pratt CB, Belasco JB, Pritchard J, Malpas JS, Baker AR, Kirkpatrick JA, *et al*: The effect of adjuvant chemotherapy on relapse-free survival in patients with osteosarcoma of the extremity. *N Engl J Med* 314: 1600-1606, 1986.
- Topalian SL, Hodi FS, Brahmer JR, Gettinger SN, Smith DC, McDermott DF, Powderly JD, Carvajal RD, Sosman JA, Atkins MB, *et al*: Safety, activity, and immune correlates of anti-PD-1 antibody in cancer. *N Engl J Med* 366: 2443-2454, 2012.
- Yang Y: Cancer immunotherapy: Harnessing the immune system to battle cancer. *J Clin Invest* 125: 3335-3337, 2015.
- Gattinoni L, Powell DJ Jr, Rosenberg SA and Restifo NP: Adoptive immunotherapy for cancer: Building on success. *Nat Rev Immunol* 6: 383-393, 2006.
- Mellman I, Coukos G and Dranoff G: Cancer immunotherapy comes of age. *Nature* 480: 480-489, 2011.
- Shionoya Y, Kanaseki T, Miyamoto S, Tokita S, Hongo A, Kikuchi Y, Kochin V, Watanabe K, Horibe R, Saijo H, *et al*: Loss of tapasin in human lung and colon cancer cells and escape from tumor-associated antigen-specific CTL recognition. *Oncoimmunology* 6: e1274476, 2017.
- Toor SM and Elkord E: Therapeutic prospects of targeting myeloid-derived suppressor cells and immune checkpoints in cancer. *Immunol Cell Biol* 96: 888-897, 2018.
- Salgado R, Denkert C, Demaria S, Sirtaine N, Klauschen F, Pruneri G, Wienert S, Van den Eynden G, Baehner FL, Penault-Llorca F, *et al*: The evaluation of tumor-infiltrating lymphocytes (TILs) in breast cancer: Recommendations by an international TILs working group 2014. *Ann Oncol* 26: 259-271, 2015.
- Mantovani A and Sica A: Macrophages, innate immunity and cancer: Balance, tolerance, and diversity. *Curr Opin Immunol* 22: 231-237, 2010.
- Fridman WH, Pagès F, Sautès-Fridman C and Galon J: The immune contexture in human tumours: Impact on clinical outcome. *Nat Rev Cancer* 12: 298-306, 2012.
- Rodell CB, Arlauckas SP, Cuccarese MF, Garris CS, Li R, Ahmed MS, Kohler RH, Pittet MJ and Weissleder R: TLR7/8-agonist-loaded nanoparticles promote the polarization of tumour-associated macrophages to enhance cancer immunotherapy. *Nat Biomed Eng* 2: 578-588, 2018.
- Phanstiel DH, Van Bortle K, Spacek D, Hess GT, Shamim MS, Machol I, Love MI, Aiden EL, Bassik MC and Snyder MP: Static and dynamic DNA loops form AP-1-bound activation hubs during macrophage development. *Mol Cell* 67: 1037-1048.e6, 2017.
- Demaria O, Cornen S, Daëron M, Morel Y, Medzhitov R and Vivier E: Publisher correction: Harnessing innate immunity in cancer therapy. *Nature* 576: E3, 2019.
- Chao MP, Weissman IL and Majeti R: The CD47-SIRPα pathway in cancer immune evasion and potential therapeutic implications. *Curr Opin Immunol* 24: 225-232, 2012.
- Liu X, Pu Y, Cron K, Deng L, Kline J, Frazier WA, Xu H, Peng H, Fu YX and Xu MM: CD47 blockade triggers T cell-mediated destruction of immunogenic tumors. *Nat Med* 21: 1209-1215, 2015.
- Advani R, Flinn I, Popplewell L, Forero A, Bartlett NL, Ghosh N, Kline J, Roschewski M, LaCasce A, Collins GP, *et al*: CD47 blockade by Hu5F9-G4 and rituximab in non-Hodgkin's lymphoma. *N Engl J Med* 379: 1711-1721, 2018.
- Munn DH and Bronte V: Immune suppressive mechanisms in the tumor microenvironment. *Curr Opin Immunol* 39: 1-6, 2016.
- Noy R and Pollard JW: Tumor-associated macrophages: From mechanisms to therapy. *Immunity* 41: 49-61, 2014.
- Chen Q, Wang C, Zhang X, Chen G, Hu Q, Li H, Wang J, Wen D, Zhang Y, Lu Y, *et al*: In situ sprayed bioresponsive immunotherapeutic gel for post-surgical cancer treatment. *Nat Nanotechnol* 14: 89-97, 2019.
- Komohara Y, Fujiwara Y, Ohnishi K and Takeya M: Tumor-associated macrophages: Potential therapeutic targets for anti-cancer therapy. *Adv Drug Deliv Rev* 99: 180-185, 2016.
- Gordon S and Martinez FO: Alternative activation of macrophages: Mechanism and functions. *Immunity* 32: 593-604, 2010.

29. Huang B, Zhao J, Li H, He KL, Chen Y, Chen SH, Mayer L, Unkles JC and Xiong H: Toll-like receptors on tumor cells facilitate evasion of immune surveillance. *Cancer Res* 65: 5009-5014, 2005.
30. De Schutter T, Andrei G, Topalis D, Duraffour S, Mitera T, van den Oord J, Matthys P and Snoeck R: Reduced tumorigenicity and pathogenicity of cervical carcinoma SiHa cells selected for resistance to cidofovir. *Mol Cancer* 12: 158, 2013.
31. Grauer OM, Molling JW, Bennink E, Toonen LW, Suttmuller RP, Nierkens S and Adema GJ: TLR ligands in the local treatment of established intracerebral murine gliomas. *J Immunol* 181: 6720-6729, 2008.
32. Hagelueken G, Clarke BR, Huang H, Tuukkanen A, Danciu I, Svergun DI, Hussain R, Liu H, Whitfield C and Naismith JH: A coiled-coil domain acts as a molecular ruler to regulate O-antigen chain length in lipopolysaccharide. *Nat Struct Mol Biol* 22: 50-56, 2015.
33. Wynn TA, Chawla A and Pollard JW: Macrophage biology in development, homeostasis and disease. *Nature* 496: 445-455, 2013.
34. Kim J and Bae JS: Tumor-associated macrophages and neutrophils in tumor microenvironment. *Mediators Inflamm* 2016: 6058147, 2016.
35. Zhang QW, Liu L, Gong CY, Shi HS, Zeng YH, Wang XZ, Zhao YW and Wei YQ: Prognostic significance of tumor-associated macrophages in solid tumor: A meta-analysis of the literature. *PLoS One* 7: e50946, 2012.
36. Weilbaecher KN, Guise TA and McCauley LK: Cancer to bone: A fatal attraction. *Nat Rev Cancer* 11: 411-425, 2011.
37. World Medical Association: World medical association declaration of Helsinki: Ethical principles for medical research involving human subjects. *JAMA* 310: 2191-2194, 2013.
38. Sui C, Wu Y, Zhang R, Zhang T, Zhang Y, Xi J, Ding Y, Wen J and Hu Y: Rutin inhibits the progression of osteoarthritis through CBS-mediated RhoA/ROCK signaling. *DNA Cell Biol* 41: 617-630, 2022.
39. He P, Hu Y, Huang C, Wang X, Zhang H, Zhang X, Dai H, Wang R and Gao Y: N-butanol extract of *gastrodia elata* suppresses inflammatory responses in lipopolysaccharide-stimulated macrophages and complete Freund's adjuvant-(CFA-) induced arthritis rats via inhibition of MAPK signaling pathway. *Evid Based Complement Alternat Med* 2020: 1658618, 2020.
40. Gordon S: Alternative activation of macrophages. *Nat Rev Immunol* 3: 23-35, 2003.
41. Mohanty S, Aghighi M, Yerneni K, Theruvath JL and Daldrup-Link HE: Improving the efficacy of osteosarcoma therapy: Combining drugs that turn cancer cell 'don't eat me' signals off and 'eat me' signals on. *Mol Oncol* 13: 2049-2061, 2019.
42. Feng M, Chen JY, Weissman-Tsakamoto R, Volkmer JP, Ho PY, McKenna KM, Cheshier S, Zhang M, Guo N, Gip P, *et al.*: Macrophages eat cancer cells using their own calreticulin as a guide: Roles of TLR and Btk. *Proc Natl Acad Sci USA* 112: 2145-2150, 2015.
43. Singel KL and Segal BH: NOX2-dependent regulation of inflammation. *Clin Sci (Lond)* 130: 479-490, 2016.
44. Tsuchiya H, Kanazawa Y, Abdel-Wanis ME, Asada N, Abe S, Isu K, Sugita T and Tomita K: Effect of timing of pulmonary metastases identification on prognosis of patients with osteosarcoma: The Japanese musculoskeletal oncology group study. *J Clin Oncol* 20: 3470-3477, 2002.
45. Palucka AK and Coussens LM: The basis of oncoimmunology. *Cell* 164: 1233-1247, 2016.
46. Raval RR, Sharabi AB, Walker AJ, Drake CG and Sharma P: Tumor immunology and cancer immunotherapy: Summary of the 2013 SITC primer. *J Immunother Cancer* 2: 14, 2014.
47. Pardoll DM: The blockade of immune checkpoints in cancer immunotherapy. *Nat Rev Cancer* 12: 252-264, 2012.
48. Jiang X, Wang J, Deng X, Xiong F, Ge J, Xiang B, Wu X, Ma J, Zhou M, Li X, *et al.*: Role of the tumor microenvironment in PD-L1/PD-1-mediated tumor immune escape. *Cancer* 18: 10, 2019.
49. Constantinidou A, Alifireris C and Trafalis DT: Targeting programmed cell death-1 (PD-1) and ligand (PD-L1): A new era in cancer active immunotherapy. *Pharmacol Ther* 194: 84-106, 2019.
50. Quamine AE, Olsen MR, Cho MM and Capitini CM: Approaches to enhance natural killer cell-based immunotherapy for pediatric solid tumors. *Cancers (Basel)* 13: 2796, 2021.
51. Wang RF and Wang HY: Immune targets and neoantigens for cancer immunotherapy and precision medicine. *Cell Res* 27: 11-37, 2017.
52. Callea M, Albiges L, Gupta M, Cheng SC, Genega EM, Fay AP, Song J, Carvo I, Bhatt RS, Atkins MB, *et al.*: Differential expression of PD-L1 between primary and metastatic sites in clear-cell renal cell carcinoma. *Cancer Immunol Res* 3: 1158-1164, 2015.
53. Humphries MP, McQuaid S, Craig SG, Bingham V, Maxwell P, Maurya M, McLean F, Sampson J, Higgins P, Greene C, *et al.*: Critical appraisal of programmed death ligand 1 reflex diagnostic testing: Current standards and future opportunities. *J Thorac Oncol* 14: 45-53, 2019.
54. Shin DS, Zaretsky JM, Escuin-Ordinas H, Garcia-Diaz A, Hu-Lieskovan S, Kalbasi A, Grasso CS, Hugo W, Sandoval S, Torrejon DY, *et al.*: Primary resistance to PD-1 blockade mediated by JAK1/2 mutations. *Cancer Discov* 7: 188-201, 2017.
55. Syn NL, Teng MWL, Mok TSK and Soo RA: De-novo and acquired resistance to immune checkpoint targeting. *Lancet Oncol* 18: e731-e741, 2017.
56. Sau S, Petrovici A, Alsaab HO, Bhise K and Iyer AK: PDL-1 antibody drug conjugate for selective chemo-guided immune modulation of cancer. *Cancers (Basel)* 11: 232, 2019.
57. Vonderheide RH: CD47 blockade as another immune checkpoint therapy for cancer. *Nat Med* 21: 1122-1123, 2015.
58. Theruvath J, Menard M, Smith BAH, Linde MH, Coles GL, Dalton GN, Wu W, Kiru L, Delaidelli A, Sotillo E, *et al.*: Anti-GD2 synergizes with CD47 blockade to mediate tumor eradication. *Nat Med* 28: 333-344, 2022.
59. Willingham SB, Volkmer JP, Gentles AJ, Sahoo D, Dalerba P, Mitra SS, Wang J, Contreras-Trujillo H, Martin R, Cohen JD, *et al.*: The CD47-signal regulatory protein alpha (SIRP $\alpha$ ) interaction is a therapeutic target for human solid tumors. *Proc Natl Acad Sci USA* 109: 6662-6667, 2012.
60. Perry CJ, Muñoz-Rojas AR, Meeth KM, Kellman LN, Amezcua RA, Thakral D, Du VY, Wang JX, Damsky W, Kuhlmann AL, *et al.*: Myeloid-targeted immunotherapies act in synergy to induce inflammation and antitumor immunity. *J Exp Med* 215: 877-893, 2018.
61. Wiehagen KR, Girgis NM, Yamada DH, Smith AA, Chan SR, Grewal IS, Quigley M and Verona RI: Combination of CD40 agonism and CSF-1R blockade reconditions tumor-associated macrophages and drives potent antitumor immunity. *Cancer Immunol Res* 5: 1109-1121, 2017.
62. Mohanty S, Yerneni K, Theruvath JL, Graef CM, Nejadnik H, Lenkov O, Pisani L, Rosenberg J, Mitra S, Cordero AS, *et al.*: Nanoparticle enhanced MRI can monitor macrophage response to CD47 mAb immunotherapy in osteosarcoma. *Cell Death Dis* 10: 36, 2019.
63. Luo Z, Li P, Deng J, Gao N, Zhang Y, Pan H, Liu L, Wang C, Cai L and Ma Y: Cationic polypeptide micelle-based antigen delivery system: A simple and robust adjuvant to improve vaccine efficacy. *J Control Release* 170: 259-267, 2013.
64. Bocanegra Gondan AI, Ruiz-de-Angulo A, Zabaleta A, Gómez Blanco N, Cobaleda-Siles BM, García-Granda MJ, Padro D, Llop J, Arnaiz B, Gato M, *et al.*: Effective cancer immunotherapy in mice by polyIC-imiquimod complexes and engineered magnetic nanoparticles. *Biomaterials* 170: 95-115, 2018.
65. Soto-Pantoja DR, Terabe M, Ghosh A, Ridnour LA, DeGraff WG, Wink DA, Berzofsky JA and Roberts DD: CD47 in the tumor microenvironment limits cooperation between antitumor T-cell immunity and radiotherapy. *Cancer Res* 74: 6771-6783, 2014.



This work is licensed under a Creative Commons Attribution-NonCommercial-NoDerivatives 4.0 International (CC BY-NC-ND 4.0) License.